BIRCHES and Lunarcubes: Building the First Deep Space Cubesat Broadband IR Spectrometer

Pamela Clark*[a], Robert MacDowall[b], William Farrell[b], Cliff Brambora[b], Terry Hurford[b], Dennis Reuter[b], Eric Mentzell[b], Deepak Patel[b], Stuart Banks[b], David Folta[b], Noah Petro[b], Benjamin Malphrus[c], Kevin Brown[c], Carl Brandon[d], Peter Chapin[d]

[a]California Institute of Technology Jet Propulsion Laboratory, 4800 Oak Grove Drive, Pasadena, CA 91109; [b]NASA Goddard Space Flight Center, 8800 Greenbelt Road, Greenbelt, MD 20771; [c]Morehead State University, Space Science Center, Morehead, KY 40351; [d]Vermont Technical College, Randolph Center, VT 05061

*Pamela.E.Clark@jpl.nasa.gov; phone 1 818 393-3262; fax 1 818 354-8887; jpl.nasa.gov

ABSTRACT

The Broadband InfraRed Compact High-resolution Exploration Spectrometer (BIRCHES), which will be described in detail here, is the compact broadband IR spectrometer of the Lunar Ice Cube mission. Lunar Ice Cube is one of 13 6U cubesats that will be deployed by EM1 in cislunar space, qualifying as lunarcubes. The LunarCube paradigm is a proposed approach for extending the affordable CubeSat standard to support access to deep space via cis-lunar/lunar missions. Because the lunar environment contains analogs of most solar system environments, the Moon is an ideal target for both testing critical deep space capabilities and understanding solar system formation and processes. Effectively, as developments are occurring in parallel, 13 prototype deep space cubesats are being flown for EM1. One useful outcome of this 'experiment' will be to determine to what extent it is possible to develop a lunarcube 'bus' with standardized interfaces to all subsystems using reasonable protocols for a variety of payloads. The lunar ice cube mission was developed as the test case in a GSFC R&D study to determine whether the cubesat paradigm could be applied to deep space, science requirements driven missions, and BIRCHES was its payload. Here, we present the design and describe the ongoing development, and testing, in the context of the challenges of using the cubesat paradigm to fly a broadband IR spectrometer in a 6U platform, including minimal funding and extensive need for leveraging existing assets and relationships on development, the foreshortened schedule for payload delivery on testing, and minimum bandwidth translating into simplified or canned operation.

Keywords: cubesat, broadband IR, lunarcubes, lunar orbiter, 6U, EM1

1. INSTRUMENT OVERVIEW

The versatile GSFC-developed payload BIRCHES (**Figure 1**), Broadband (1 to 4 micron) InfraRed Compact, High-resolution Exploration Spectrometer, is a miniaturized version of OVIRS (Osiris-Rex Visible InfraRed Spectrometer) on OSIRIS-Rex **[1]**. BIRCHES is a compact (1.5U, 2 kg, 12-25 W) point spectrometer with a compact cryocooled HgCdTe focal plane array for broadband measurements. The instrument includes an IRIS/AIM microcryocooler and controller **[2]**. The instrument will achieve sufficient SNR (>100) and spectral resolution (10 nm) through the use of a Linear Variable Filter to characterize and distinguish several spectral features associated with water in the 3-micron region, and potentially other volatiles already detected by LCROSS (H_2S, NH_3, CO_2, CH_4, OH, organics) and mineral bands. Typical footprint size will be 10 x 10 km, but will be somewhat smaller at the equator and larger toward the poles. We are also developing compact instrument electronics that can be easily reconfigured to support future instruments with Teledyne H1RG focal plane arrays **[1]** in 'imager' mode, when the communication downlink bandwidth becomes available. The instrument will enable the Lunar Ice Cube (**Figure 2**) mission science goals: determination of composition and distribution of volatiles in lunar regolith as a function of time of day, latitude, regolith age and composition, and thus enable understanding of current dynamics of lunar volatile sources, sinks, and processes, with implications for evolutionary origin of volatiles.

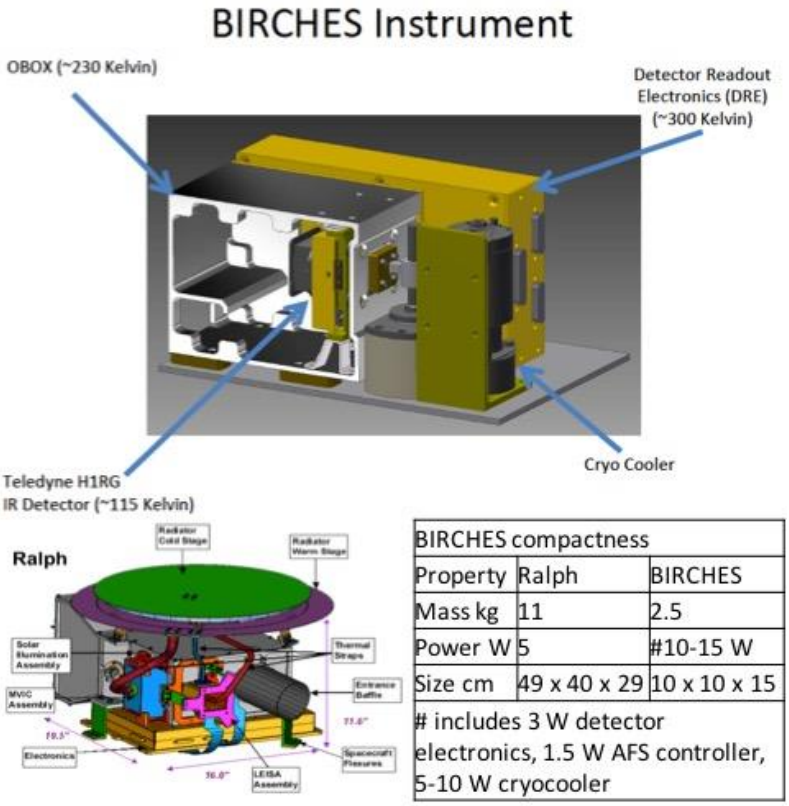

BIRCHES compactness		
Property	Ralph	BIRCHES
Mass kg	11	2.5
Power W	5	#10-15 W
Size cm	49 x 40 x 29	10 x 10 x 15
# includes 3 W detector electronics, 1.5 W AFS controller, 5-10 W cryocooler		

Figure 1: BIRCHES (top) a miniaturized version of the LEISA line of instruments including the much larger New Horizons Ralph (bottom) and the subsequent OSIRIS Rex OVIRS from which it has direct heritage.

We focus here on the nature of and strategies for BIRCHES design and development: in six key areas 1) compact, simplified optics; 2) compact electronics, including controllers and Digital Readouts (DREs), capable of surviving over a year in deep space, using strategies to minimize bandwidth, with DREs supporting the H1RG family of focal plane arrays with minor modification; 3) incorporation of the microcryocooler and controller; 4) thermal and mechanical design capable of maintaining detector and optics box at required temperatures; 5) operation in the lunar environment; and 6) interface with the spacecraft.

2. SCIENCE CONTEXT

The year 2009 was a very exciting time for lunar research, with two major findings regarding water at the Moon: the Lunar Crater Observation Sensing Satellite (LCROSS) observation of abundant water and ice released from the floor of polar crater Cabeus **[3] [4]**. Instruments onboard Chandrayaan, EPOXI, and Cassini unexpectedly detected an IR spectral absorption feature indicating the presence of an OH veneer extending from poles to equator and apparently varying with latitude or longitude **[5] [6] [7]**. These findings suggest that the Moon has both water and OH diurnal cycles that are not yet fully verified and understood.

Despite earlier tantalizing evidence for water ice in permanently shadowed craters **[8] [9] [10] [11] [12] [13]**, the observation of OH surface veneer at mid to low latitude regolith at 10-1000 ppm **[5]** was considered quite surprising given past Apollo sample analysis **[14]**. Apparent Mare Imbrium regional decrease in surface OH at local noon suggests a diurnal effect **[6]** (**Figure 3**). This dynamic indicates a possible exogenic solar wind source for hydroxylation **[15] [5] [6].** However, noon-time at Mare Imbrium is also the time when the Moon is located in the geomagnetic tail and no longer in the solar wind. Thus, the apparent decrease in OH may be related to tail passage as opposed to thermal desorption losses. The cause of the OH decrease effect remains unsolved. McCord and coworkers **[14]** examined the possible sources of the OH veneer, and concluded that the complex array of sources, especially feldspathic mineralogy

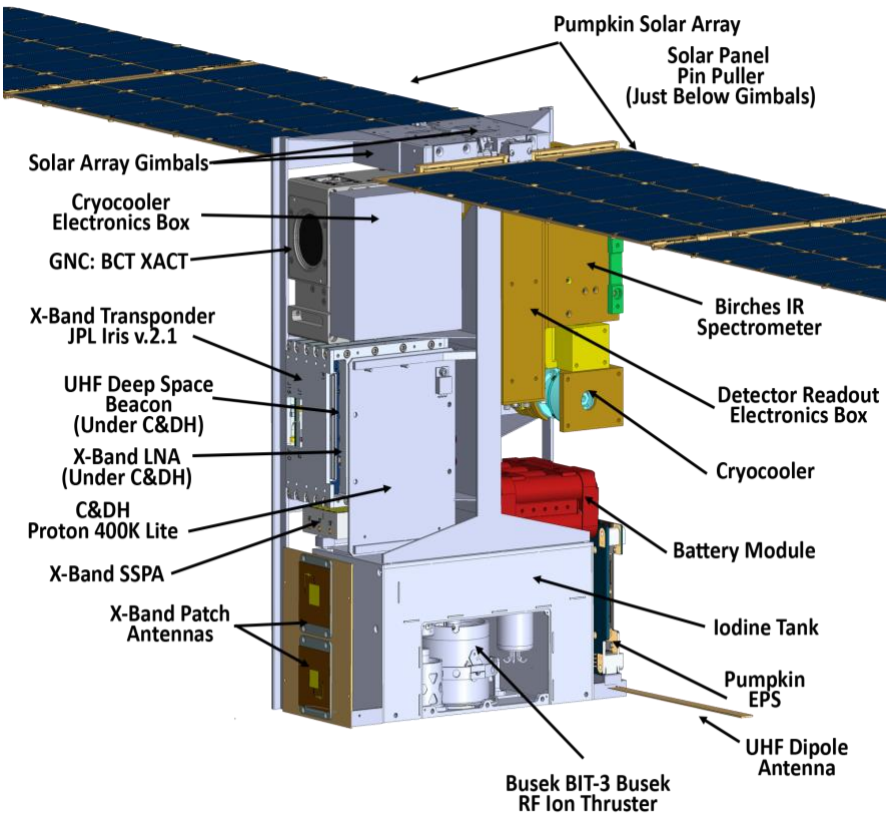

Figure 2: Compact configuration of Lunar Ice Cube bus with BIRCHES spectrometer nadir pointing in upper left.

and solar wind implantation, act simultaneously to account for the observed absorption. Kramer and coworkers **[13] [16]** found that the local IR OH absorption feature was reduced (less OH content) in swirl regions associated with magnetic anomalies. The finding suggests that hydroxylation is locally reduced where the B-field also blocks solar wind propagation onto the surface **[16] [17]**.

In response, BIRCHES is designed to provide the basis for determining the forms and sources of lunar volatiles in spectral, temporal, spatial, and geological context by:

- being flown as the Lunar Ice Cube mission payload in a low equatorial periselene, nearly polar, highly elliptical lunar orbit with repeating coverage at different times of day during several lunar cycles,

- being capable, unlike previous orbiting spectrometers, of analysis that encompasses not only many features associated with water and other volatiles, but the broad 3-micron band associated with water species (**Table 1, Figure 4**),

- utilizing data obtained from previous missions (**Table 2**), such as composition, regolith age, terrane, and slope, and by calibrating its results for the same volatile or mineralogical features obtained from previous observations to provide geological and geochemical context.

In this way, Lunar Ice Cube will achieve its primary goal: to measure the water components (weak physi-adsorbed OH, strong chemi-adsorbed OH, molecular water, ice) as a function of lunation, solar zenith angle, slope, and surface properties as a means of addressing the NASA HEOMD Strategic Knowledge Gap of understanding the distribution and transportation of water on the Moon as a means of enabling potential resource prospecting. Measuring the abundance and distribution of water and water components is also crucial for determining whether OH and water sources are interior, chemogenic, or exterior.

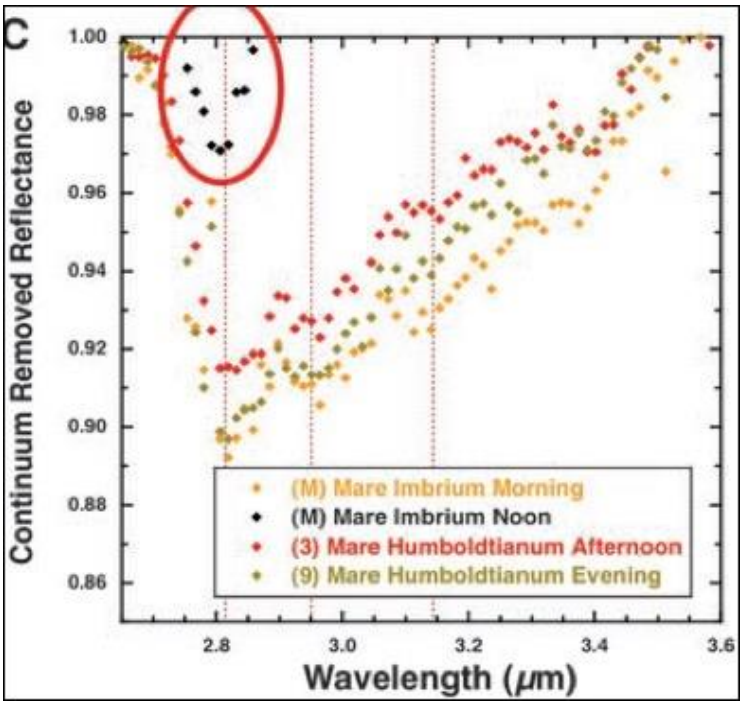

Figure 3: Early evidence for diurnal variation trend in OH absorption [6], which will be geospatially linked by BIRCHES.

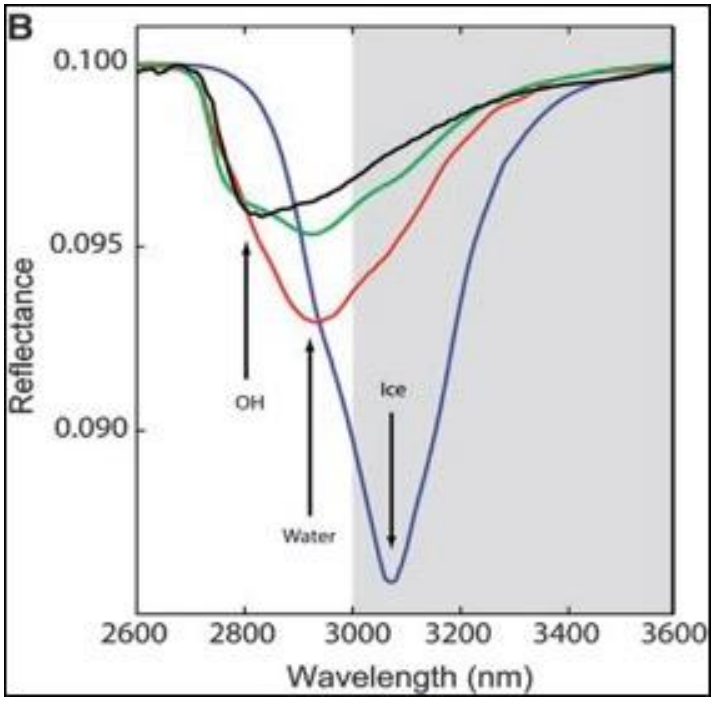

Figure 4: BIRCHES measurements do not cut off [5] but encompass the broad 3 micron band to distinguish overlapping OH, water, and ice features.

Table 1 Spectral Bands in detector range with Water-related bands in and around the 3 micron region highlighted.

Species	Wavelength µm	Description
Water form, component		
water vapor	2.738	OH stretch
	2.663	OH stretch
liquid water	3.106	H-OH fundamental
	2.903	H-OH fundamental
	1.4	OH stretch overtone
	1.9	HOH bend overtone
	2.85	M3 Feature
	2.9	total H2O
hydroxyl ion	2.7-2.8	OH stretch (mineral)
	2.81	OH (surface or structural) stretches
	2.2-2.3	cation-OH bend
	3.6	structural OH
bound H2O	2.85	[24] [18]
	3	H2O of hydration
	2.95	H2O stretch (Mars)
	3.14	feature w/2.95
adsorbed H2O	2.9-3.0	R. Clark [25] [19]
ice	1.5	band depth-layer correlated
	2	strong feature
	3.06	[3] [5]
Other Volatiles		
NH3	1.65, 2. 2.2	N-H stretch
CO2	2, 2.7	C-O vibration and overtones
H2S	3	
CH4/organics	1.2, 1.7, 2.3, 3.3	C-H stretch fundamental and overtones
Mineral Bands		
pyroxene	0.95-1	crystal field effects, charge transfer
olivine	1, 2, 2.9	crystal field effects
spinels	2	crystal field effects
iron oxides	1	crystal field effects
carbonate	2.35, 2.5	overtone bands
sulfide	3	conduction bands
hydrated silicates	3-3.5	vibrational processes
anticipate wavelength of peak for water absorption band to be structural<bound<adsorbed<ice		

Table 2 Lunar Ice Cube BIRCHES builds on previous missions.

Mission	Finding	Lunar Ice Cube
Cassini VIMS, Deep Impact	surface water detection, variable hydration, with noon peak absorption	water and other volatiles, fully characterize 3 µm region as function of several times of day for same swaths over range of latitudes w/ context of regolith mineralogy and maturity, radiation and particle exposure, for correlation w/ previous data
Chandrayaan M3	H2O and OH (<3 microns) in mineralogical context nearside snapshot at one lunation	
LCROSS	ice, other volatile presence and profile from impact in polar crater	
LP, LRO (LEND LAMP, DVNR, LOLA, LROC), LADEE	H+ in first meter (LP, LEND) & at surface (LAMP) inferred as ice abundance via correlation with temperature (DIVINER), PSR and PFS (LROC, LOLA), H exosphere (LADEE)	

3. HERITAGE

BIRCHES, is a broadband, flexible, cubesat-scale IR spectrometer concept, flyable as a point or imaging spectrometer as bandwidth allows (point spectrometer for this application due to bandwidth limitations), with heritage from OSIRIS-REx (Origins Spectral Interpretation Resource Identification and Security-Regolith Explorer) OVIRS (OSIRIS-REx Visible InfraRed Spectrometer) and New Horizons LEISA (Linear Etalon Imaging Spectral Array) **[20] [21] [22]**. BIRCHES represents a compact version of a family of simple, versatile, and low-cost instruments, adapted as OSIRIS Rex OVIRS is adapted, from the GSFC-developed LEISA (Ralph) **[20] [21] [22] [1]** (**Figure 1**). LEISA-derived instruments represent (lower cost, mass, volume, power) concepts in spectrometer design made possible by large-format infrared detectors combined with advances in thin-film technology in the form of non-dispersive thin film filters, called wedged or linear variable etalon filters (LVE or LVF), as wavelength selection elements. Such spectrometers represent a great reduction in optical and mechanical complexity and volume compared to conventional grating, prism, or Fourier transform spectrometers and mechanically or electrically tunable filter systems. As a cubesat instrument with minimal funding, BIRCHES requires extensive leveraging via utilization of:

- Teledyne H1RG Focal Plane Array with a linear variable filter, both spares from OVIRS.
- Thermally isolated, compact optics, designed and developed as GSFC internal R&D for cubesat, inner solar system version of OVIRS
- AIM Microcryocooler developed for AFRL being tested on Lunar Ice Cube for deep space
- H1RG generic compact detector interface electronics with flexible architecture suitable for point or imaging spectrometers leveraging ongoing NASA/GSFC internal R&D efforts to developed mixed signal ASICs.

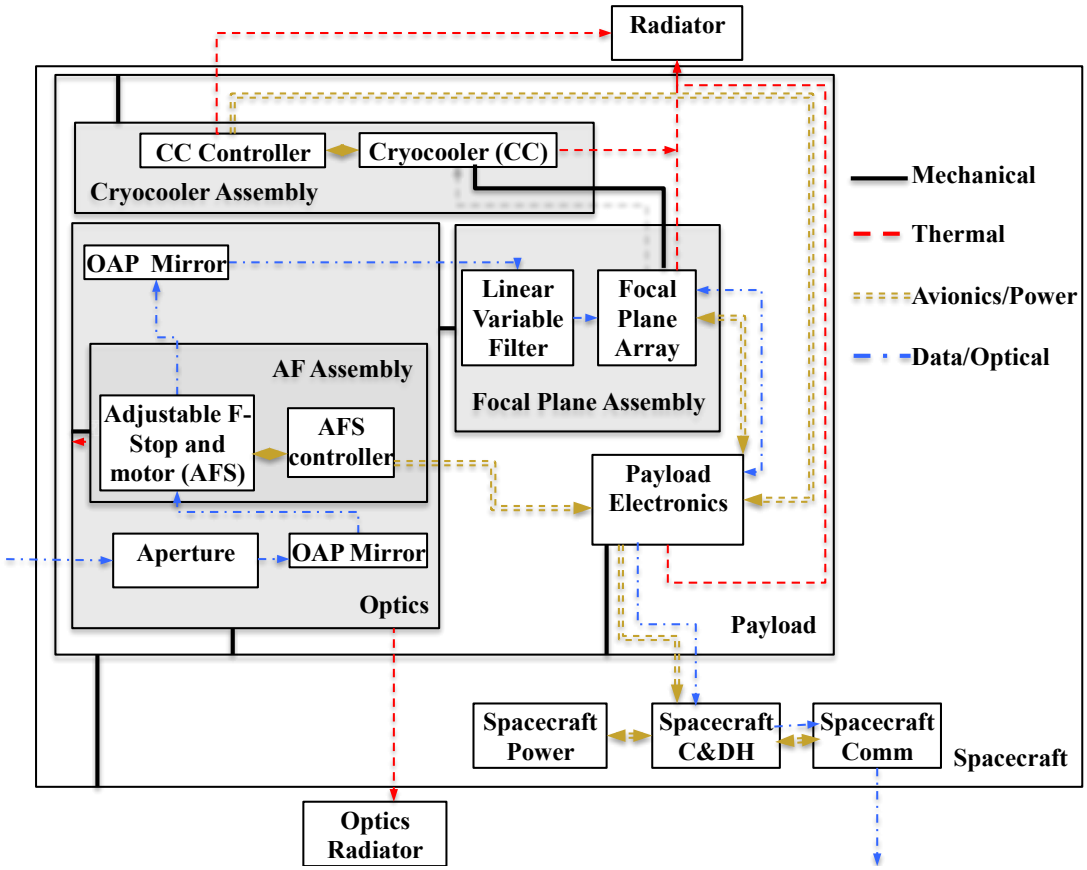

Figure 5: BIRCHES schematic illustraitng subsystems and their interfaces and simplicity of design and mechanical, avionics, data, and thermal interfaces with the bus.

4. INSTRUMENT SUBSYSTEMS

4.1 Optics and Optical Components

The BIRCHES optics (**Figures 1 and 5**), consists of the Optical Box (OBOX) enclosure with the 4 cm aperture, two off-axis parabolic mirrors (OAP) with a field stop consisting of an Adjustable Field Stop (AFS) between them, the Linear Variable Filter (LVF) mounted on the Teledyne H1RG detector, and an effective field of view of 6 degrees. The LVF is a wedged progressive band pass filter: the peak wavelength transmitted in a given position varies as a function of the variable thickness. As can be seen in Figure 1a, all components are attached to the enclosure, which includes baffles, and the mirrors are all of aluminum construction to minimize the impact of temperature changes.

The AFS allows flexibility, for maintaining spot size regardless of altitude or controlling (maximizing or minimizing) spot size in response to changes in altitude. Consisting of two overlapping leaves with 90 degree notches, the AFS opening is adjusted by a two phase stepper motor with electronic controls in the Detector Readout Electronics (DRE), The BIRCHES adjustable field stop, which can vary the footprint area by a factor of >5, will be used in conjunction with the variable integration time, which can be >/= 0.5 seconds, to 1) minimize saturation closer to the subsolar point and maximize SNR near to the terminators, and 2) assure that footprint area is </= 100 square kilometers. The 0.5 second integration period combined with the approximately 2.5 km/sec along-track velocity allows us to obtain up to 8 frames for the nominal 10 km along-track footprint. The spacecraft ACS system will allow the BIRCHES instrument to maintain the required nadir pointing, to maintain less than 10% variation in coverage from the projected footprint (5% or 0.5 km in x and y directions). The drivers are knowledge and control at the greater altitude (1000 km at terminator). To achieve this goal, our ACS system provides <0.5 milliradians control of pointing (equivalent to 0.5 km at 1000 km) with knowledge of <0.05 milliradians., meeting our requirements.

The original cryocooler was deemed unacceptable due to excessive vibration. The original cryocooler electronics were found to be unacceptable for use from a radiation tolerance perspective. Replacements were the far lower jitter IRIS/AIM cryocooler and its more radiation tolerant and compact controller. This IRIS/AIM cryocooler/controller package had the additional advantage of a smaller volume footprint. In addition, the original AFS was too large to fit within the BIRCHES volume allocation. The newly designed, more compact AFS that allows BIRCHES to fit within the volume allocation is nearing completion at GSFC.

Optical alignment and testing of the BIRCHES instrument will be similar to the OVIRS instrument, its direct antecedent. We will align the elements in phases where each phase progressively improves alignment to the limit of its capability. The process starts with a system coordinate system definition and a “rough alignment” phase for each component, where the elements are aligned using mechanical metrology to 0.1 millimeter. The second, mid-range phase ends with elements aligned to μm and arc seconds using opto-mechanical metrology techniques (e.g., interferometry) and alignment fiducials. The third, and final, phase ends with the system alignment optimized such that the wavefront error is measured in nanometers and is dominated by fabrication errors on the mirrors. As a backup plan, if the performance requirements are met, indicating no active re-alignment is necessary, then the third phase will simply be a calibration of the wavefront error. Some sub-components will require pre-calibration before installation into the system. The AFS, for example, will require a sub-system level characterization in which the opening and center will be measured independently. The opening will be calibrated by measuring the opening and comparing it to the AFS readout of the position sensor. Interferometric measurements will require a floating optical table sufficient in size to accommodate the optics assembly and the required hardware. Other alignment work not involving the interferometer can be accomplished on a solid granite or standard optics table. BIRCHES will be tested and calibrated under space-like conditions in a small thermal vacuum chamber with an external heated plate adjusted to simulate the thermal signature BIRCHES will experience under mission conditions.

4.2 Thermal and Mechanical Systems

Lunar orbit is one of the more thermally challenging environments in the solar system. In addition, BIRCHES has special thermal requirements: variations in temperature associated with the optics during observations must be minimized and the detector must be kept cold (see below). Thus, when we originally considered using BIRCHES in this environment, we began by looking at the thermal design and determining if, with the exception of the microcryocooler, all else could be done passively. We looked at a passive thermal design which included two radiators and other conventional elements. The largest radiator, covering one (3U x 1U) panel of the spacecraft with four G10 thermal isolator shims to support and isolate it from the adjacent chassis panels and cryocooler radiator, is a radiator for the optics box alone. The other smaller radiator is dedicated to the cryocooler and the DRE. First order modeling (for our

worst-case scenario orbit including coverage of subsolar and midnight) indicates that this design maintains the optics box at the required <220±5 K during science data taking (minimizing thermal noise above 3 μm) as long as the radiator is not pointed at the sun. (Our 'worst case' orbit is 100 km periapsis above subsolar point with a 2-hour eclipse through lunar midnight). In order for the cryocooler to control the detector to 115±1 K the sink for cryocooler radiator must be maintained between 0_o and 40_o C, which our model indicates is achievable with margin. The spacecraft will be rotated around nadir as necessary to minimize exposure of the optics box radiator to the sun. Other thermal elements include the MLI blanket to protect the instrument from parasitic heat from the spacecraft and reflective white paint on radiator surfaces. Further testing as part of this program will refine and increase confidence in our thermal models.

A thermal test will be performed to validate the thermal model through thermal balance testing. Thermal vacuum cycling is required to verify the functionality of the hardware cycling through extreme temperatures. Once the model is correlated, the design can be put through multiple scenarios and show predictions through analysis.

4.3 Cryocooler and Controller

For years, space flight cryocooler development has concentrated on ultra-low vibration and long life, resulting in large, heavy, expensive coolers, typically incorporating linear pressure wave generators with two opposed pistons driven by linear motors. Recently, several groups have experimented with different approaches to make more compact cryocoolers suitable for miniaturized instruments, including Ricor, Lockheed Martin, and IRIS/AIM. We originally considered the very inexpensive Ricor 562S tactical cooler, a compact version of the K508 used on JPL Mars lander missions [23], which converts the rotary motion of a single high torque 3-phase DC brushless motor to the linear motion of the compressor piston and displacer by using a crankshaft, connecting rods and ball bearings and allowing for a more compact short stroke-large bore geometry. This configuration has historically provided high efficiency in terms of mass, power and size compared to linear coolers but at the cost of higher vibration, and shorter life. Recent advances in bearing technology and motor drive technique have allowed for a further reduction in moving mass. The increased need for micro coolers to support UAV and handheld targeting scopes has brought forward a new generation of micro-rotary coolers with this innovation. Due to the lower moving mass, and tighter bearing tolerances, this generation of rotary coolers offers significantly reduced noise and vibration as well as increased operational life compared to earlier versions. However, the combination of still noticeable jitter, and particularly the lack of radiation tolerance of the Ricor controller made this selection untenable. Instead, we will be using the 'third generation' IRIS/AIM SX030 single piston linear cooler with its compact and efficient miniaturized low cost microcryocooler electronics already developed for the US Air Force. It has improved cooling capacity (0.6W @ 140K), a moderately larger profile with the cryocooler electronics, cryocooler pump, and separate cold finger assembly, but far less jitter and a far more radiation tolerant controller.

We believe the IRIS/AIM SX030 [2] and controller will meet our requirement to maintain the detector at <115±1K using from 5 to 10 W of onboard power. IRIS/AIM already complies with the original GEVS based vibration requirements. Slightly more aggressive vibe requirements (below 2K) have been recently announced for the EM1 cubesats. IRIS/AIM is looking at these updated requirements to establish compliance. Thermal performance of the system will be confirmed during Instrument level thermal vacuum testing at NASA/GSFC prior to delivery.

The cooler features a single temperature sensor in the cold tip, which will provide telemetry for the temperature of the tip, and the thermal strap leading to the detector. The detector itself has a temperature sensor within the Read Out Integrated Circuit (ROIC) which will provide telemetry for the detector temperature. A third temperature sensor will be attached to the OBOX to provide telemetry data for that part of the instrument. In order to permit unattended, autonomous operation of the cryocooler and to ensure a high degree of repeatability in the thermal and vibration characterization tests, as part of the GSE design, GSFC personnel will have the ability to monitor and shutdown the cooler under any out-of-bound conditions.

4.4 Detector Assembly

BIRCHES utilizes an existing (at GSFC) Teledyne H1RG Mercury Cadmium Telluride (HgCdTe) 18 μm pixel (pitch) 2D focal point array (FPA) with associated Linear Variable Filter (LVF) originally built as spares for OSIRIS Rex OVIRS (**Figure 6**) [1]. OVIRS uses a 512 x 512 pixel region of a 1024 x 1024 FPA. The H1RG arrays are constructed by hybridizing (via Indium bump bonds) a photosensitive HgCdTe detector layer, with the appropriate Hg/Cd ratio, to a CMOS Read Out Integrated Circuit (ROIC). The array substrate is removed, allowing photon sensitivity over the entire range and also reducing the effect of spurious signals from cosmic rays. The LVF, a proven and compact means of line separation, is an etalon, deposited on one surface as a substrate as described **[20]**. Etalon thickness and therefore transmitted wavelength varies as a function of position. Reflective surfaces of the etalon are formed by stacks of

dielectric layers with maximum reflectivities that have the same wavelength dependence as the etalon thickness. The thickness of the dielectric layers is controlled by a machined mask that rotates in front of the substrate, allowing the positional dependence of the wavelength and/or the wavelength dependence of the resolution to be tailored to specific applications. BIRCHES utilizes three (out of the five provided by OVIRS) 102 x 512 pixel wedged filter segments bound together in a single assembly and mounted within 1 mm of the FPA surface. The wavelength of transmitted light varies along the 512-pixel row. Each 102 pixel column corresponds to a single spectral element, and a full spectrum is created using data from all the columns. Pixels within a column are summed to increase the signal-to-noise ratio. Because the wavelength may vary somewhat along a column, only those pixels in each column lying near the central wavelength of appropriate spectral range will be summed. The central wavelength of each pixel will be determined during ground calibration. Resolving power and resolution vary as a function of wavelength. Resolution is 10 nm and resolving power 350 between 2.9 and 3.6 μm, surrounding the critical 3 μm band, well within the state-of-the art.

4.5 Detector Readout (Interface) Electronics

We utilize our compact generic DRE, designed to be easily reconfigurable for point or imaging spectrometer for the family of Teledyne HCT HnRG spectrometers, combined with heritage from our ongoing IRAD work on low cost,

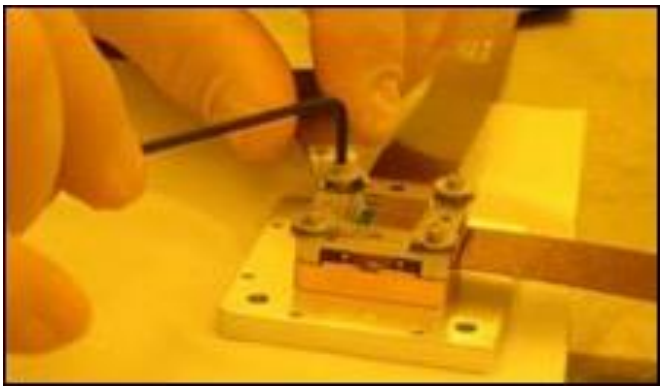

Figure 6: BIRCHES utilizes a compact Teledyne HgCdTe FPA (H1RG) and JDSU linear variable filter detector assembly, leveraging OSIRIS Rex OVIRS.

compact electronics, to meet the performance and compact volume requirements. Both of these are challenging requirements primarily due to the compact nature of the design.

After a short initial period of requirements definition, leveraging current work on generic detector interface electronics design, we are developing the BIRCHES electronics from TRL 4 (Technology concept and/or application formulation) to TRL 6 (Fully integrated with operational hardware/software systems) by refining the requirements for the design, creating a schematic which supports the required functions to support the detector interfaces (including the AFS and microcryocooler control interfaces), creating a layout for the compact (~2.5" x 4") Printed Wiring Boards (PWBs), procuring the PWB and EEE (Electrical, Electronic, and Electromechanical) parts, assembling the PWB, and testing the assembly with the Teledyne H1RG detector to demonstrate compliance with card and instrument requirements. A modified version of the OVIRS Flexible Printed Wiring (FPW) cryo-detector harness will be used during the testing. This modified harness design will also be used for the flight instrument.

The DRE features a dual channel commercially available ADC converter and a PRO-ASIC-III FPGA to stimulate the detector with the appropriate biases and clocking schemes, digitize up to two outputs from the detector, gather the samples from the A/D converters, collect them, average them as required to reduce the data rate to better match the expected down link allocation (~128 kbps), and format the results into a packet format for transmission off the board via LVTTL based communication interfaces to the GSE (Ground Support Equipment) computer for storage and analysis. The electronics will be packaged in an Aluminum enclosure designed to meet vibration and thermal requirements.

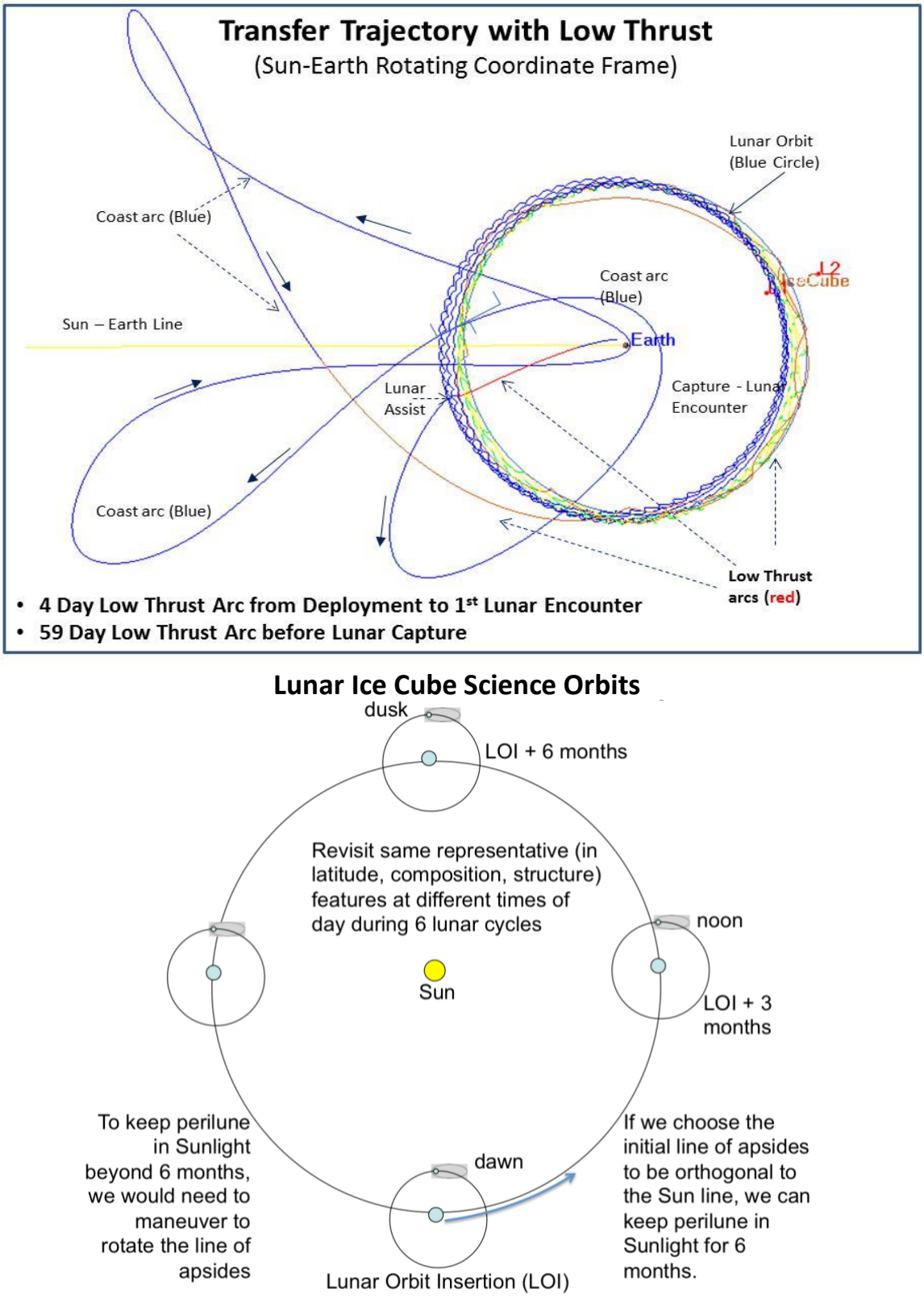

Figure 7. Lunar Ice Cube utilizes a minimal DV transfer trajectory (top) harnessing expertise of GSFC flight dynamics to achieve lunar capture. After 3 months of periapsis lowering, the nearly polar, highly elliptical science orbit (bottom) achieves a repeating pattern, providing coverage of the same features for up to 6 different times of day (once per lunar cycle).

5. SCIENCE INVESTIGATION

Science data-taking with the BIRCHES payload will occur in two phases, following the approximately 9-month journey on a low energy trajectory initiated at EM1 deployment. Phase 1 will occur between lunar capture and the science orbit, Phase 2 (**Figure 7**) during the highly elliptical science orbit (100 km x 5000 km, equatorial periapsis, nearly polar), with a repeating coverage pattern that provides overlapping coverage at different lunations. During phase 1, translational propulsion burns are occurring during major portions of most orbits in order to progressively lower periapsis and achieve the desirable incidence angle. Periodically (up to once a week), an orbit will be used for instrument calibration and capture of spectral signatures for larger portions of the lunar disk, traversing from terminator to terminator. Particular attention will be paid to systematic or solar activity dependent transient effects resulting from charged particle interactions around the terminators. Once the nominal full science orbit is achieved, phase 2 will begin, and the main propulsion system will no longer be required. Phase 2, the 'science mission' will last approximately 6 months, 6 lunar cycles, allowing for sufficient collection of systematic measurements as a function of time of day to allow derivation of volatile cycle models.

Prior to flight, Detector response will be measured over its entire spectral range (1 to 4 microns) using a standard radiometric source over a range of intensities under simulated mission conditions (in thermal vacuum). Spectral calibration for the entire system will be accomplished using gratings to provide effective monochromatic scanned radiometric sources with R>2,000. Radiometric and relative spectral response calibrations will be performed using NIST traceable calibrated blackbodies and flood sources. The quality of the point-spread function will be assessed using collimated point and extended sources. The boresight pointing will be measured with respect to an optical alignment cube. From these calibrations, nominal corrections for dark current, spatial or spectral non-linearity, and temperature will be derived for the instrument.

During flight, periodic calibration will be performed to monitor instrument performance and update instrument calibration parameters. Although linear Variable (wedged) filters have very stable spectral response, spectral calibration will be performed redundantly by comparison of BIRCHES spectra with known star spectra and infrared reflectance spectra from prior missions including M3 on Chandrayaan **[24] [25] [26]** acquired under comparable (time of day, nadir pointing) conditions, with particular attention paid to calibration sites at a variety of latitudes utilized by earlier orbital missions, especially the Apollo 16 site conventionally used for infrared reflectance calibration if overlapping coverage is available. We will utilize the approach of Pieters and coworkers **[24]** for comparing dissimilar spectrometers using a common wavelength and observations at the same phase angle and latitude. This approach has been shown to be capable of demonstrating linearity in radiance values. Dark current and background flux will be measured using dark sky observations periodically during the non-illuminated portion of the orbit. Although the thermal design will constrain temperature variation during data taking as described below, the optics box temperature will be monitored and based on earlier laboratory calibrations, temperature corrections will be applied as necessary.

Table 3: Total signal, reflectivity, SNR, and predictd absorption depths as a function of ppm water in the 3 micron band for 4 different locations relative to the subsolar point [5] [27] [28].

Case	Lat	ToD	Temp K	Total Signal/Reflectivity @ 3um photons/sec		SNR	Band depth/PPM water		
							0.1 @ 1000	0.05 @ 500	0.01 @ 100
1	0	+/-6.2	163	3254	2760	52	276	138	27
2	60	0 noon	335	39045	26400	162	2640	1320	264
3	20	+/-4.3	304	24279	20963	145	2096	1480	210

6. RADIOMETRY

BIRCHES will detect incoming radiation from lighted reflected off of the lunar surface (our 'measurement'), thermal emission from the lunar surface and thermal emission from detector surfaces. Absorption features will be superimposed on the reflectance measurement. Radiometric plots for our instrument configuration, assuming 4 cm aperture and 6-degree field of view (**Table 3**, **Figure 8**) indicate that lunar surface emission does not become significant at temperatures within the instrument according to our thermal models until beyond the three-micron band. Emission from detector

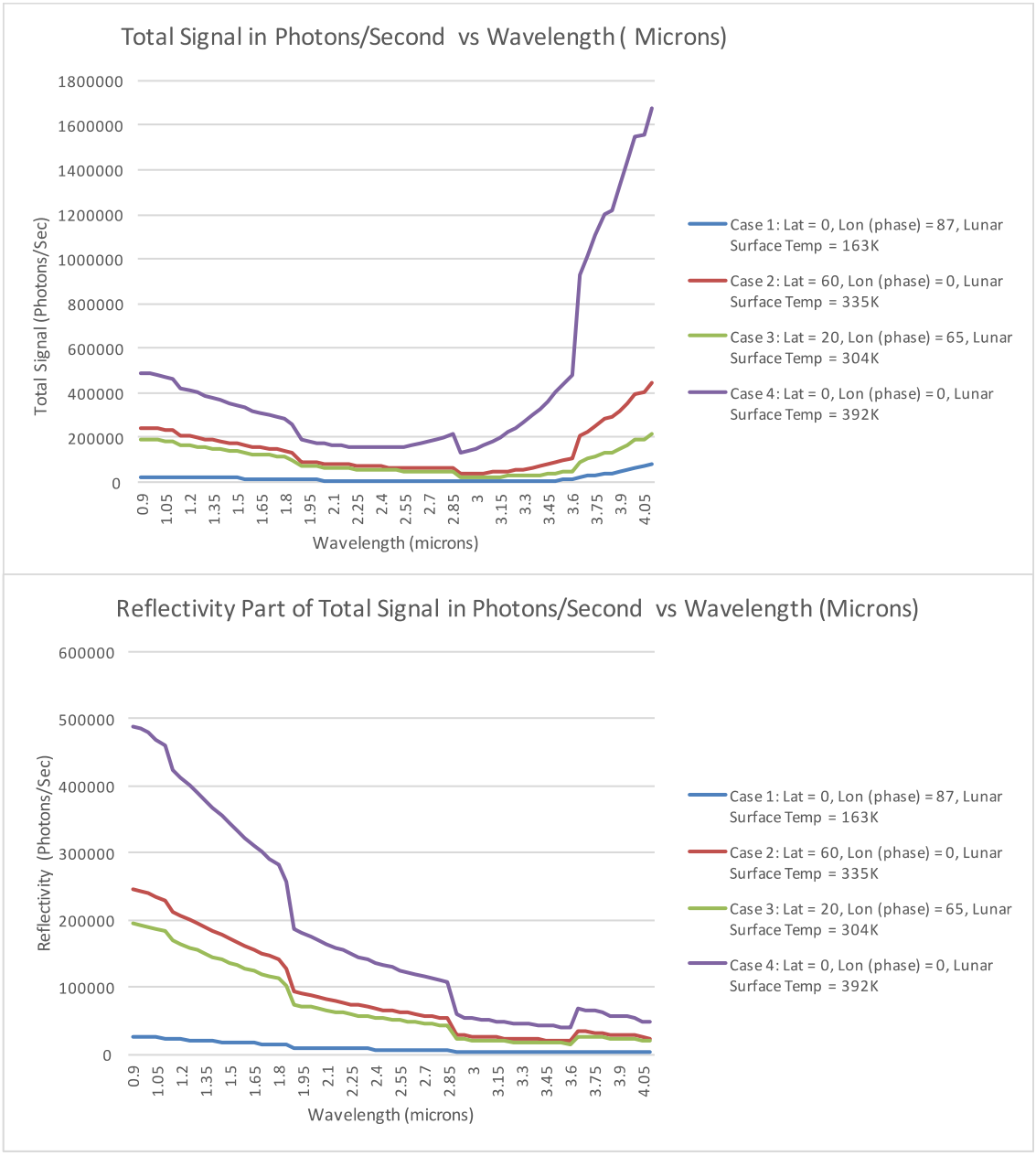

Figure 8: Radiometry models for total signal and reflectivity indicating that thermal emission does not become significant until beyond the three-micron band and that SNR required to see absorption features should be adequate even as the terminators are approached (see text). Also see Table 3.

surfaces remains a minor component regardless of wavelength. These models also allow us to remove thermal emission as a function of wavelength. In addition, for the three-micron band, we should have adequate signal to noise ratio (SNR) to see the absorption features even as we approach the terminator as long as water abundance is at the hundredths of a percent level or above.

7. CURRENT STATUS

About 3 months from CDR, and a year from delivery of our payload to Morehead State for integration with the 6U bus, our current progress is as follows:

1) Design and testing on the detector electronics is complete at GSFC. Detector readout algorithm is nearly complete. Detector electronics now include the adjustable field stop controller and an interface for microcryocooler control.

2) To compensate for more volume needed by the detector electronics and for the replacement for the original microcryocooler, we needed a more compact optics box. Final design work is complete on the optics box, which includes a compact adjustable field stop.

3) Testing on the IRIS/AIM microcryocooler and its controller is nearly completed.

4) High fidelity thermal modeling of the completed instrument model is underway.

8. ACKNOWLEDGMENT

This research was carried out at the Jet Propulsion Laboratory, California Institute of Technology, under a contract with the National Aeronautics and Space Administration.

REFERENCES

[1] Reuter, D. and A. Simon-Miller, "The OVIRS Visible/IR Spectrometer on the OSIRIS-REx Mission," Lunar and Planetary Science, 1074.pdf (2012)
[2] Ellis, M., T. Luong, L. shaw, J. Murphy, E. Moody, A. Lisiecki, C. Kirkconnell, "Development of a miniature cryocooler system for cubesats", Cryocoolers, 18, 329-337 (2014).
[3] Colaprete, A., P. Schultz, J. Heldmann, D. Wooden, M. Shirley, K. Ennico, B. Hermalyn, W. Marshall, A. Ricco, R. Elphic, D. Goldstein, D. Summy, "Detection of Water in the LCROSS Ejecta Plume," Science, 330, 463-468 (2010).
[4] Schultz, P., B. Hermalyn, A. Colaprete, K. Ennico, M. Shirley, W. Marshall, "The LCROSS cratering experiment," Science, 330, 6003, 468-472 (2010).
[5] Pieters, C., J. Boardman, B. Burtti, A. Chatterjee, R. Clark, T. Glavich, R. Green, J. Head, P. Isaacson, E. Malaret, T. McCord, J. Mustard, N. Petro, C. Runyon, M. Staid, J. Sunshine, L. Taylor, S. Tompkins P. Caranasi, M. White, "Character and spatial distribution of OH/H2O on the Moon seen by M3 on Chandrayaan-1," Science, 326, 568-572 (2009).
[6] Sunshine, J. M., T. L. Farnham, L. M. Feaga, O. Groussin, F. d. r. Merlin, R. E. Milliken, and M. F. A'Hearn, "Temporal and Spatial Variability of Lunar Hydration As Observed by the Deep Impact Spacecraft," *Science*, *326*, 565-578 (2009).
[7] Clark, R., "Detection of Adsorbed Water and Hydroxyl on the Moon, *Science*," **326**, 562-564 (2009).
[8] Watson, K., H. Brown, B. Murray, "On possible presence of ice on the Moon," 66, 5,1598-1600 (1961).
[9] Watson, K., B. Murray, H. Brown, "The Stability of volatiles in the solar system," Icarus, 1, 317-327 (1963).
[10] Arnold, J.R., "Ice in the lunar polar regions," JGR, 84, NB10, 5659-5668 (1979).
[11] Lanzerotti, L.J., "Ice in the polar regions of the Moon," JGR, 86, B5, 3949-3950 (1981).
[12] Feldman, W., S. Maurice, A. Binder, B. Barraclough, R. Elphic, D. Lawrence, "Fluxes of fast and epithermal neutrons from lunar prospector: Evidence for water ice at the lunar poles," Science, 281, 5382, 1496-1500 (1998).
[13] Goddard, Robert H., In *Papers of Robert H. Goddard, Volume I*, eds; E. C. Goddard & G. E. Pendray (New York: McGraw-Hill, 1970), pp. 413-430 (1920).
[14] McCord, T. B., L. A. Taylor, J.-P. Combe, G. Kramer, C. M. Pieters, J. M. Sunshine, and R. N. Clark, "Sources and physical processes responsible for OH/H2O in the lunar soil as revealed by the Moon Mineralogy Mapper (M3)," Journal of Geophysical Research, 116, E6, E00G05 (2011).
[15] Zeller, E., L. Ronca, P. Levy "Proton-induced hydroxyl formation on the lunar surface," JGR Planets, 71, 4855-4860 (1966).
[16] Kramer, G., S. Besse, D. Dhingra, J. Nettles, R. Klima, I. Garrick-Bethel, R. Clark, J.-P. Combe, J. Head, L. Taylor, C. Pieters, J. Boardman, T. McCord, "M3 spectral analysis of lunar swirls and the link between optical maturation and surface hydroxyl formation at magnetic anomalies," JGR Planets, 116, E00G18 (2011).

[17] Poppe, A., J. Halekas, G. Delory, W. Farrell, "Particle-in-cell simulations of the solar wind interaction with lunar crustal magnetic anomalies: magnetic cusp regions," JGR Space Physics, 117, A09105 (2012).
[18] Houck, J., J. Pollack, C. Sagan, D. Schaack, J. Decker, "High altitude Infrared spectroscopic evidence for bound water on Mars, Icarus, 18, 470-480 (1973).
[19] Clark, R.N., Spectral Properties of Mixtures of Montmorillonite and Dark Carbon Grains: Implications for Remote Sensing Minerals Containing Chemically and Physically Adsorbed Water, *JGR Planets.* **88,** 10635-10644 (1983).
[20] Reuter, D., A. Stern, J. Scherrer, D. Jennings, J. Baer, J. Haney, L. Hardaway, A. Lunsford, S. McMuldroch, J. Moore, C. Olkin, R. Parizek, H. Reitsma, D. Sabatke, J. Spencer, J> Stone, H. Throop, J. VanCleve, G. Weigle, L. Young, "Hyperspectral sensing using the Linear Etalon Imaging Spectral Array," SPIE Proceedings, 2597, Advanced and Next-generation Satellites II, 154 (1997).
[21] Reuter, D., A. Stern, J. Baer, L. Hardaway, D. Jennings, S. McMuldroch, J. Moore, C. Olkin, R. Parizek, D. Sabatke, J. Scherrer, J. Stone, J. VanCleve, L. Young, "Ralph: A visible/infrared imager for the New Horizons Pluto/Kuiper Belt Mission", SPIE Proceedings of the Optics and Photonics Conference, Astrobiology and Planetary Missions, 5906-51, 59061F-1 to 59061F-11, 5906-51 (2005).
[22] Reuter, D., A. Stern, J. Scherrer, D. Jennings, J. Baer, J. Hanley, L. Hardaway, A. Lunsford, S. McMuldroch, J. Moore, C. Olkin, R. Parizek, H. Reitsma, D. Sabatke, J. Spencer, J. Stone, H. Throop, J. VanCleve, G. Weigle, L. Young, "Ralph: A visible/infrared imager for the New Horizons Pluto/Kuiper Belt Mission," Space Science Reviews, 140, 1-4, 129-154 (2008
[23] Johnson, D., M. Lysek, J. Morookian, "The Ricor K508 cryocooler operational experience on Mars", AIP Conf Proc, 1573, 1792 (2017).
[24] Pieters, C. M., J. Boardman, M. Ohtake, T. Matsunaga, J. Haruyama, R. Green, U. Mali, M. Staid, P. Isaacson, Y. Yokota, S. Yamamoto, S. Besse, J. Sunshine, "One Moon, many measurements 1: radiance values," Icarus, 226, 1, 951-963 (2013).
[25] Ohtake, M., C. Pieters, P. Isaacson, S. Besse, Y. Yokota, T. Matsunaga, J. Boardman, S. Yamamota, J. Haruyama, M. Staid, U. Mall, R. Green, "One Moon, many measurements 3: Spectral reflectance," Icarus, 226, 1, 364-374 (2013).
[26] Besse, S., Y. Yokota, J. Boardman, R. Green, J. Haruyama, P. Isaacson, U. Mall, T. Matsunaga, M. Ohtake, C. Pieters, M. Staid, J. Sunshine, S. Yamamoto, "One Moon, many measurements 2: Photometric corrections," Icarus, 226, 127-139 (2013).
[27] Milliken, R., J. Mustard, F. Poulet, D. Jouglet, J.-P. Bibring, B. Gondet, Y. Langevin, "Hydration state of the Martian surface as seen by Mars Express OMETA: H2o content of the surface", JGR Planets, 112, E08S07.
[28] Milliken, R., J. Mustard, "Estimating the water content of hydrated minerals using reflectance spectroscopy: effects of darkening agenst and low-aledo materials", Icarus, 189, 550-573 (2007).